Ruthenium Phthalocyanine and Its Reaction with Dioxygen: Synthesis, Structure, Magnetism, and Electrical Conductivity Properties of the Cofacially Assembled Ruthenoxane Aggregate of Formula HO−[(Pc)RuO]$_n$−H (Average n = 11)

A. Capobianchi,[†] G. Pennesi,[†] A. M. Paoletti,[†] G. Rossi,*[,†] R. Caminiti,[‡,§] C. Sadun,[‡,§] and C. Ercolani[§]

ICMAT (CNR), Area della Ricerca di Roma, CP 10, 00016 Monterotondo Stazione, Italy, and Istituto Nazionale per la Fisica della Materia (INFM) and Dipartimento di Chimica, Università La Sapienza, p.le A. Moro 5, 00185 Roma, Italy

Received December 27, 1995[⊗]

Reaction of $(PcRu)_2$ with dioxygen under a variety of conditions leads in all cases to a solid amorphous oxygen-containing aggregate formulated as HO−[(Pc)RuO]$_n$−H. Detailed structural information on this material has been obtained by the large-angle X-ray scattering technique (LAXS). It has been established that the aggregate consists of −(Pc)Ru^{IV}−O− fragments (the best fitting between experimental and calculated data requiring average n = 11), linked together by linear Ru^{IV}−O−Ru^{IV} bridges, with Ru(IV) in the center of the planar Pc ring and in-plane Ru−N$_{Pc}$ and out-of-plane Ru−O bond distances of 1.923 and 1.845 Å, respectively. The Pc rings are cofacially assembled with an inter-ring spacing of 3.69 Å, staggering (35°) and eclipsing of the rings alternating along the stacking direction. Additional information on the structure and electronic state of this ruthenoxane material has been obtained by IR, resonance Raman, EPR, ESCA, and magnetic susceptibility studies. Its stability as a solid and in a solution of H_2SO_4 has also been examined. The room-temperature electrical conductivity of the solid, σ_{RT}, is 1×10^{-2} Ω^{-1} cm^{-1}. This value is discussed in the light of the reported values for $(PcRu)_2$ and other similar metalloxane aggregates.

Introduction

Exploration of the synthesis, chemical physical properties, and reactivity of ruthenium phthalocyanine derivatives appears not to have been so far adequately extended,[1a−d] expecially if compared with that of some first transition series metal phthalocyanines.[2] We recently established,[1a] by the LAXS (large-angle X-ray scattering) technique, that ruthenium phthalocyanine, obtained as an amorphous material from the adduct [PcRu(DMSO)$_2$]·2DMSO,[1e] is dimeric, $(PcRu)_2$ (Ru−Ru bond distance: 2.40 Å). The solid state structure of the complex has been shown to consist of columnarly stacked molecular units resulting in an aggregate of formula $[(PcRu)_2]_n$ (average n = 6; Figure 1). The structural information obtained for this material has provided the basis for a reasonable explanation of its magnetic behavior as well as of its electrical conduction properties ($\sigma_{RT} = 1 \times 10^{-5}$ Ω^{-1} cm^{-1}). It has also been observed[1a] that ruthenium phthalocyanine, when dissolved in THF, reacts with molecular oxygen, as indicated by UV−visible spectral changes. In the presence of terminal olefins, ruthenium phthalocyanine acts, in a solution of the same solvent, as a dioxygen activator and is able to oxidize catalytically and selectively 1-octene to 2-octanone.

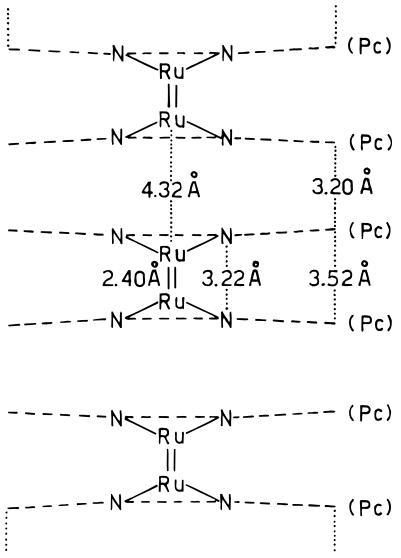

$[(PcRu)_2]_n$ (average n = 6)

Figure 1. Schematic representation of the stacking of the dimeric units in amorphous $[(PcRu)_2]_n$. Reprinted with permission from ref 1a. Copyright 1994 American Chemical Society.

It has now been observed that ruthenium phthalocyanine interacts with molecular oxygen in different media (ClNP, benzene, toluene, etc.). A solid amorphous oxygen-containing material of general formula HO−[(Pc)Ru^{IV}O]$_n$−H (**I**) is reproducibly obtained. This ruthenoxane material has been studied by the LAXS technique, and its structural features are examined here in connection with its electrical conduction properties and other information achieved by UV−visible, IR, EPR, and ESCA spectra, magnetic susceptibility data, and its behavior in concentrated H_2SO_4 (96%).

[†] ICMAT (CNR).
[‡] INFM, Università La Sapienza.
[§] Departimento di Chimica, Università La Sapienza.
[⊗] Abstract published in *Advance ACS Abstracts,* June 15, 1996.

(1) (a) Capobianchi, A.; Paoletti, A. M.; Pennesi, G.; Rossi, G.; Caminiti, R.; Ercolani, C. *Inorg. Chem.* **1994**, *33*, 4635 and references therein. (b) Nyokong, T.; Guthrie-Strachan, J. *Inorg. Chim. Acta* **1993**, *208*, 239. (c) Schmeisser, D.; Pohmer, J.; Hanack, M.; Göpel, W. *Synth. Met*. **1993**, *61*, 115. (d) Hanack, M.; Polley, R. *Inorg. Chem*. **1994**, *33*, 3201. (e) Abbreviations used in the present paper: Pc = phthalocyaninato dianion, $C_{32}H_{16}N_8^{2-}$; OEP = octaethylporphyrinato dianion; DMSO = dimethyl sulfoxide; quin = quinoline; py = pyridine; ClNP = α-chloronaphthalene.
(2) (a) *Phthalocyanines—Properties and Applications*; Leznoff, C. C., Lever, A. B. P., Eds.; VCH Publishers: New York; Vols. 1−4. (b) Moser, F. H.; Thomas, A. L. *The Phthalocyanines;* CRC, Boca Raton, FL, 1983; Vols 1 and 2.

S0020-1669(95)01667-3 CCC: $12.00

Experimental Section

DMSO, ClNP, benzene, toluene, and 96% H_2SO_4 were pure solvents. $[PcRu(DMSO)_2]\cdot 2DMSO$ was prepared by the method previously reported[3] and later used by us.[1a,4] $[PcRu(py)_2]$ and $[PcRu(quin)_2]$ were obtained from the DMSO adduct, by suspending the latter in the appropriate N-base and maintaining the suspension at the boiling temperature for a few hours. The solid was then isolated by filtration, washed with benzene, and dried under vacuum to constant weight. The polymer $[(Pc)SiO]_n$ was prepared as described elsewhere.[5]

$[PcRu]_2$. This complex was obtained by elimination of DMSO from the adduct $[PcRu(DMSO)_2]\cdot 2DMSO$ by heating under vacuum (330 °C, 10^{-2} mmHg).[3,4] As obtained, $(PcRu)_2$ shows good elemental analyses for C, H, and N. All the samples examined, however, even if freshly prepared and checked within a few days, show a little content of oxygen (1.0−1.5%), very likely due to traces of oxygen-containing contaminants irreversibly formed during the drastic elimination of DMSO. $(PcRu)_2$ could also be obtained from the quinoline and pyridine adducts as described elsewhere.[6]

Reaction of $(PcRu)_2$ with O_2. $(PcRu)_2$ (500 mg) is suspended in ClNP (20 mL) and the mixture heated in presence of O_2 or air, at 150 °C for 15 h, under stirring. After cooling and filtration, the solid material is washed abundantly with acetone and then brought to constant weight under vacuum (450 mg, ca. 90% yield). Anal. Calcd for the formula $HO-[(Pc)RuO]_n-H$ (average $n = 11$; **I**): C, 60.89; H, 2.59; N, 17.75; O, 2.77. Found (for a typical sample): C, 60.4; H, 2.35; N, 17.4; O, 3.9. The oxygen content found, slightly higher than expected, is a common feature of at least 15 different samples examined (3.5−4.5%). This result is not surprising, in the light of what has been said about the oxygen content for samples of $(PcRu)_2$. **I** can also be obtained from $(PcRu)_2$ by suspending the latter in benzene or toluene in the presence of O_2 or air and refluxing the mixture more than 48 h. $(PcRu)_2$ is recovered unchanged if suspended in ClNP, benzene, or toluene, in an inert atmosphere (N_2), under experimental conditions identical to those used for the preparation of the ruthenoxane material.

I is indefinitely stable in air. In an inert atmosphere (N_2) the material is stable up to a temperature of ca. 200 °C. Above this temperature, a continuous weight loss is observed, undoubtedly associated with the decomposition of the material, as shown unequivocally by the formation of phthalimide. **I** is completely insoluble in THF (where instead $(PcRu)_2$ is appreciably soluble) and in noncoordinating or low-coordinating solvents. It is also insoluble in pyridine and other similar N-bases. It can be dissolved in 96% H_2SO_4; visible solution spectra show, however, that **I** is unstable in this medium (see below).

One sample of **I** was obtained by contact of $(PcRu)_2$ with ^{18}O-enriched O_2 ($^{18}O = 70\%$). The mass spectral analysis of this sample shows no peaks for **I** or for any of the predictable monomeric constituents. Definitely, it shows peaks for the phthalimmide at *m/z* 147, 151, and 149, with relative intensity roughly in the ratio expected for the presence of ^{18}O. This further demonstrates, if necessary, the involvement of dioxygen in the oxidation process for the formation of **I**.

Analysis of I by the LAXS Technique. The large-angle X-ray scattering (LAXS) technique, useful for the investigation of the short-range order in amorphous systems,[7] has already been outlined for the analysis of amorphous $(PcRu)_2$.[1a] The metodology used here for the examination of **I** by the same technique is similar, both for the collection of X-ray data and for their fitting with the calculated data. Thus, we mention here, briefly, the static structure function $S(q)$, extracted from the experimental spectra, q being the scattering parameter, i.e. $q = (2/\hbar c)E(\sin\theta)$, where 2θ = the scattering angle, E = radiation energy, and c and $\hbar$ have their usual meanings. The energy-dispersive X-ray diffraction is here used to obtain the diffracted spectra of the materials. In the experimental procedure, outlined previously,[1a,8,9] a white X-ray beam source was used (tungsten; high voltage = 45 kV, current = 35 mA). Measurement angles (θ): 26, 21, 15.5, 10, 8, 5, 3, 2, 1.5, 1.2, 0.9, 0.7°. Scattering parameter interval (q): 0.3−16.82 $Å^{-1}$.

The collected data were treated as in refs 1a and 9−11. The level of the fitting of the experimental and calculated data for **I** is appropriately illustrated by function $S(q)$, graphically represented (see Figure 3) as $qS(q)\ M(q)$, with

$$M(q) = (f_{Ru}^{\ 2}(0)/f_{Ru}^{\ 2}(q))\exp(-0.01q^2) \qquad (1)$$

The Fourier transformation of the $S(q)$ functions gives the radial distribution function

$$D(r) = 4\pi r^2\rho_0 + 2r\pi^{-1}\int_0^{q_{max}} qS(q)\ M(q)\sin(rq)\ dq \qquad (2)$$

(graphically represented as $\mathrm{Diff}(r) = D(r) - 4\pi r^2\rho_0$; see Figure 4), where ρ_0 is the average electronic density of the sample [$\rho_0 = \sum_i n_i f_i(0)^2 V^{-1}$], and V is the stoichiometric volume unit chosen. A more detailed description of the noncommercial diffractometer and technique is given in refs 1a, 8, and 9.

Other Physical Measurements. IR spectra in the region 4000−200 cm^{-1} were taken on a Perkin-Elmer 16F FT-IR spectrophotometer by using Nujol mulls between CsI plates or KBr pellets. UV−visible solution spectra were recorded on a Perkin-Elmer 330 spectrophotometer. Room-temperature magnetic susceptibility measurements were obtained by the Gouy method on a permanent magnet (7000 G, 0.7 T), by using a solution of $NiCl_2$ as calibrant. X-Band EPR spectra were recorded on a Varian E-109 spectrometer; the field was calibrated with 2,2-diphenyl-1-picrylhydrazyl (DPPH). Conventional X-ray powder diffraction patterns were recorded on a Seifert 3000 instrument with a Cu Kα (50 kV, 30 mA) radiation. Elemental analyses were provided by the Servizio di Microanalisi, Area della Ricerca (CNR). Thermogravimetric analyses were performed on a DuPont 950 instrument under a stream of N_2 (0.5 $dm^3\ min^{-1}$). Dc conductivity measurements were performed at room temperature and in the range 240−40 K by the four-probe technique using powder pellets of 1.2 or 0.8 cm (diameter), pressed at ca. 10^8 Pa. Contacts were realized by silver conductive glow. Resistivity and temperature were recorded by an automatic computer program. XPS spectra were recorded on a VG ESCALAB MK2 ($p < 10^{-9}$ Torr), with an excitation source Alka (1486 eV); samples were examined as pressed pellets. The mass spectra were measured with a VG micromass 7070 F instrument (electron impact 70 eV; emission current 200 μA), located at the Servizio GC-MS, Area della Ricerca di Roma (CNR).

Results and Discussion

In our previous paper,[1a] it was unequivocally established that elimination of DMSO from the adduct $[PcRu(DMSO)_2]\cdot 2DMSO$ results in the formation of an amorphous solid material, which consists of dimeric $(PcRu)_2$ units held together by interdimer contacts to give the aggregate $[(PcRu)_2]_n$ (average $n = 6$, Figure 1). In order to prove that such a material is always formed, regardless of the nature of the adduct used, we also prepared samples of $(PcRu)_2$ from the bis(quinoline) and bis(pyridine) adducts, $[PcRu(quinoline)_2]$ and $[PcRu(pyridine)]_2$, recently reported to be also appropriate precursors of ruthenium phthalocyanine.[6] It has now been definitely established that the material obtained from these N-base adducts also consists of dimeric units and the aggregate formed is indistinguishable from that prepared from the DMSO adduct, as proved by X-ray data, IR and UV−visible spectra, magnetic behavior, and electrical conductivity properties.

(3) Kobel, W.; Hanack, M. *Inorg. Chem.* **1986**, *25*, 103.
(4) Rossi, G.; Gardini, M.; Pennesi, G.; Ercolani, C.; Goedken, V. L. *J. Chem. Soc., Dalton Trans.* **1989**, 193.
(5) Dirk, C. W.; Inabe T.; Schoch, K., Jr.; Marks, T. *J. Am. Chem. Soc.* **1983**, *105*, 1539.
(6) Hanack, M.; Osio-Barcina, J.; Witke, E; Pohmer, J. *Synthesis* **1992**, 211.
(7) Caminiti, R.; Munoz Roca, C.; Beltran-Porter, D.; Rossi, A. *Z. Naturforsch.* **1988**, *43A*, 591.
(8) (a) Caminiti, R.; Sadun, C.; Rossi, V.; Cilloco, F.; Felici, R. Paper presented at the XXVth Italian Congress on Physical Chemistry, Cagliari, Italy, 1991. (b) Patent RM/93 A000410, June 23, 1993.
(9) Caminiti, R.; Carbone, M.; Sadun, C. *J. Mater. Chem.*, in press.
(10) Fritsch G.; Keimel, D. A. *Mater. Sci. Eng.* **1991**, *A134*, 888.
(11) Nishikawa, K.; Itjima, T. *Bull. Chem. Soc. Jpn.* **1984**, *57*, 1750.

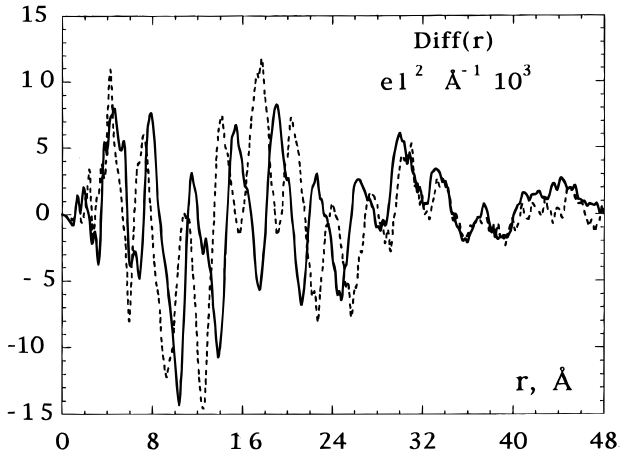

Figure 2. Experimental function Diff(r) = D(r) − $4\pi r^2\rho_0$ for $[(PcRu)_2)]_n$ (- - -) and for **I** (—).

Table 1. Final Values of the Adjusted Parameters (rms σ_{ab}) for the Model Used

$0 < r \leq 1.5$ Å	$\sigma_1 = 0.06$
$1.5 < r \leq 3.9$ Å	$\sigma_2 = 0.1$
$3.9 < r \leq 6.5$ Å	$\sigma_3 = 0.22$
$6.5 < r \leq 10$ Å	$\sigma_4 = 0.4$
$10 < r \leq 22$ Å	$\sigma_5 = 0.78$
$r > 22$ Å	$\sigma_6 = 0.9$

Structure of I. The powder X-ray diffraction patterns of samples of the ruthenoxane material **I**, obtained from different preparations, are all identical in number, shape, and relative intensity of peaks present. Instead, they are different from the spectrum of the amorphous starting $(PcRu)_2$. The observed pattern for **I** is typical of amorphous materials with a short-range order; thus, **I** has been examined by the LAXS technique. Data collection was performed on an apparatus and under experimental conditions already specified (see Experimental Section). The fitting of the experimental structure function was made by using the Debye function

$$S(q)_{ab} = \sum f_a f_b (\sin(r_{ab}q))(r_{ab}q)^{-1} \exp(-(1/2)\sigma_{ab}{}^2 q^2) \quad (3)$$

where σ_{ab} = rms variation of the distance r_{ab}. The theoretical peaks were calculated by a corresponding Fourier transformation of the theoretical intensities for the pair interactions (eq 3), using the same modification function, *M(q)* (eq 1), and the same q_{max} value (see eq 2) as for the experimental data.

The best fitting of the experimental data was facilitated primarily by the general chemical physical information available on **I**, i.e. elemental analyses, low solubility, spectra (IR, Raman, EPR, ESCA), magnetism, electrical conductivity, and spectral behavior in H_2SO_4 (see discussion below), clearly suggesting the occurrence of −(Pc)RuO− units linked to form a linearly elongated oligomer. Advantage was also taken of the following reasonably predictable structural features: (a) in-plane location and oxidation state +4 for the Ru centers; (b) rigid planarity of the Pc units; (c) possible relative rotation of adjacent Pc units.

Both the static structure function $S(q)$ and the radial distribution function Diff(r) are useful to an appropriate presentation of the obtained fitting. Preliminarly, the Diff(r) functions for $(PcRu)_2$ and **I** are given in Figure 2 for comparison. The observed marked difference between the two is indicative of the significant structural rearrangement associated with the oxidation process of the dimeric precursor. Figure 3 shows for **I** the optimized fitting for $S(q)$, and Figure 4 the corresponding graphic illustration of the radial distribution function Diff(r). Both figures indicate a very satisfactory fitting.

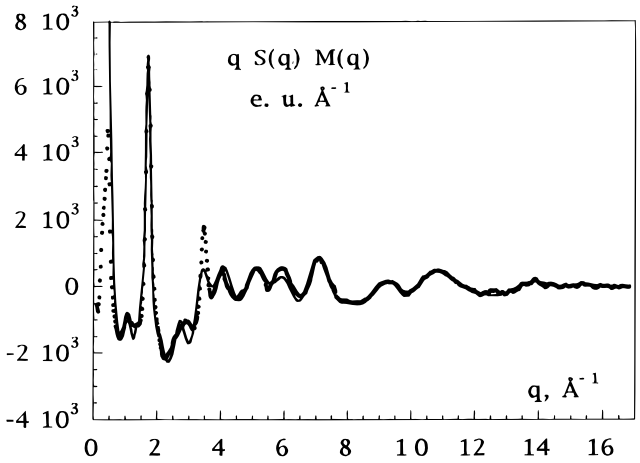

Figure 3. Observed (- - -) and calculated (—) $qS(q)$ $M(q)$ vs q for **I**.

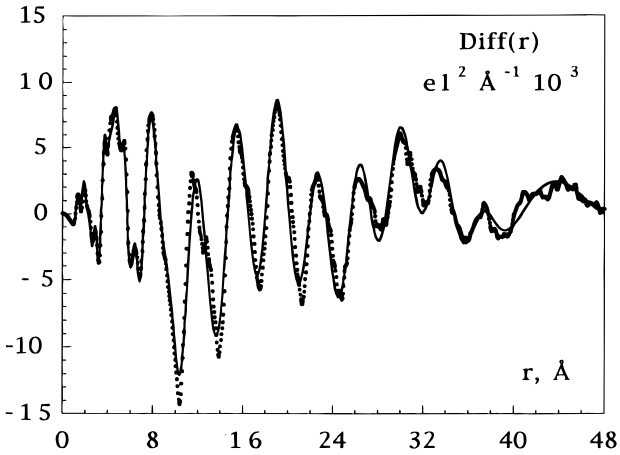

Figure 4. Experimental function Diff(r) = D(r) − $4\pi r^2\rho_0$ for **I**: experimental (- - -) and calculated data (—).

Optimization of the fitting leads to the following structural data for **I**, definitely assigned as a columnarly stacked ruthenoxane aggregate of formula HO−[(Pc)RuO]$_n$−H (schematically represented in Figure 5): (a) Ru−O and Ru−N_{Pc} bond distances 1.845 and 1.923 Å, with the Ru atom located in the center of the planar Pc unit; (b) inter-ring spacing 3.69 Å; (c) relative rotation for two adjacent Pc rings 35°; (d) n (average) = 11; (f) terminal OH groups present. All present additional information (see below), combined with the data available on similar metalloxane cofacially assembled materials, fully supports the structural assignments made for **I**.

It is particularly interesting to compare the structural features of **I** with those of the (μ-oxo)[octaethylporphyrinato]ruthenium(IV) complex of formula $[(OEP)Ru(OH)]_2O$ (**II**), known from single-crystal X-ray work,[12] and of other related metalloxane stacked polymers of general formula $[(Pc)MO]_n$ (M = Si(IV), Ge(IV), Sn(IV)).[5] Data are summarized in Table 2. **I** shares remarkable similarities with the diruthenium complex **II**, which can be thought of as a matrix subunit from which **I** might be originated (neglecting, of course, the difference in the OEP and Pc ligands). Common features are (a) linearity of the −O−Ru−O−Ru− backbone, (b) in-plane location of the central metal, (c) planarity of the MN_4 chromophoric system, and (d) staggering of adjacent macrocycles (staggering angle in **II** 19°). The internal Ru−O bond distance for **I**, 1.845 Å, is in excellent agreement with the corresponding distance found for **II** (1.847 Å) and, consequently, for the interplanar distance. The observed

(12) Masuda, H.; Taga, T.; Sugimoto, H.; Mori, M.; Ogoshi, H. *J. Am. Chem. Soc.* **1981**, *103*, 2199.

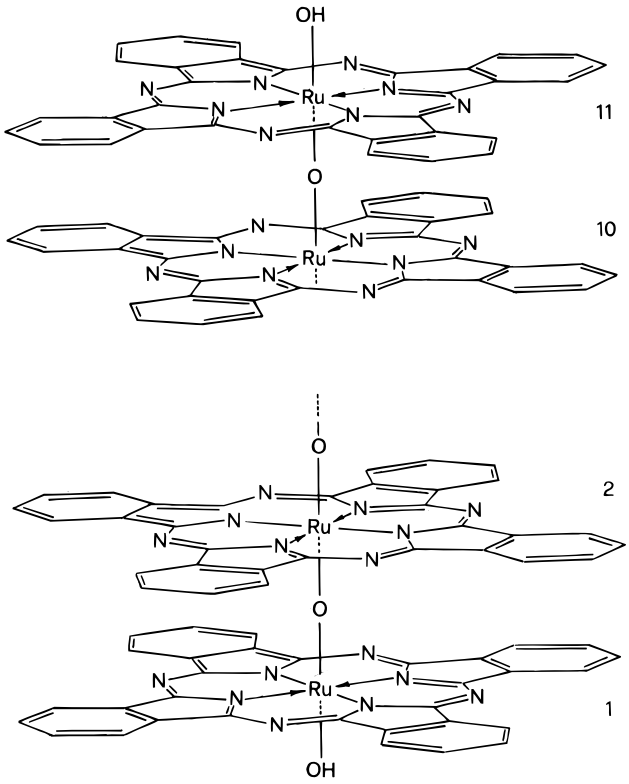

Figure 5. Schematic representation of **I**.

Table 2. Structural Data for **I** and Related Species

compd	M−O (Å)	M−O−M (Å, deg)	M−N (Å)	stagger[a] (deg)	pol deg[b] (*n*)	ref[c]
I	1.845	3.69, 180	1.923	35	11	*c*
II	1.847	3.71, 180	2.067	22.7	2	12
$[(Pc)SiO]_n$	1.65	3.33, 180		39	120 (30)	5
$[(Pc)GeO]_n$	1.77	3.55, 180		ecl	70 (40)	5
$[(Pc)SnO]_n$	1.91	3.82, 180		ecl	100 (40)	5

[a] ecl = eclipsed. [b] Degree of polymerization. [c] This paper.

marked difference between **I** and **II** in the $M-N_{Pc}$ bond distances (Table 2) can find satisfactory explanation in the different sizes of the inner N_4 chromophore of the OEP and Pc macrocycles.

Particularly interesting is also, and not merely for structural aspects (see below), the comparison of **I** with the series of cofacially assembled materials $[(Pc)MO]_n$ (M = Si(IV), Ge(IV), Sn(IV)), extensively investigated[5] as precursors of the corresponding iodine-doped electrically conductive species of formula $([(Pc)MO]I_x)$.[13] The undoped materials $[(Pc)MO]_n$ consist of linearly elongated chains built up with −(Pc)M−O− units.[5] The level of polymerization in these materials is in all cases definitely higher than the average value measured for **I** (Table 2). This probably explains their appreciable crystalline character, in contrast with the essentially amorphous nature of **I**. The data in Table 2 show that the Ru−O bond distance and the associated inter-ring spacing in **I** are intermediate between those of the Si and Ge metalloxanes and that of the Sn analog, in good agreement with expectation, on the basis of the ionic radii and positions in the periodic table of all the involved M(IV) ions.

The presence of terminal Ru−OH groups in **I** has not been unequivocally proved. Rather, it appears as a reasonable assumption, in keeping with the preparation conditions used for

(13) Diel, B. N.; Inabe, T.; Lyding, J. W.; Schoch, K. F., Jr.; Kannewurf, C. R.; Marks, T. J. *J. Am. Chem. Soc.* **1983**, *105*, 1551.

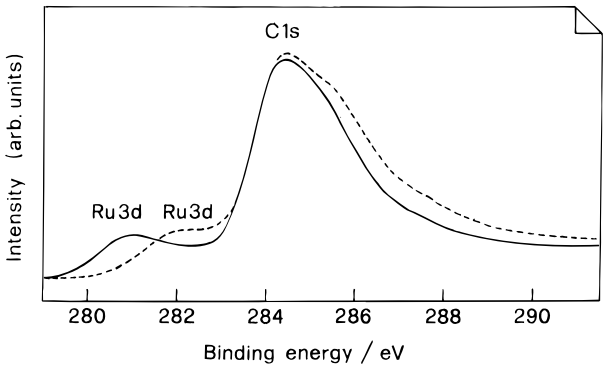

Figure 6. ESCA (XPS) spectra of $(PcRu)_2$ (—) and **I** (- - -).

I. It is also in keeping with the observed content of oxygen and the fitting of the structural data. The fitting, for instance, has shown a little progress by assuming longer terminal Ru−O bond lengths (2.19 Å, as suggested by the findings for **II**), whereas it was definitely less satisfactory if the presence of terminal five-coordinate Ru(III) centers was considered. Moreover, were this the case, it would be difficult to explain why just terminal Ru centers would cease their oxidation process halfway between Ru(II) and Ru(IV). Finally, it should be noted that the precise identification of the terminal groups in **I** is only of moderate interest for the present discussion of the main structure of this stacked material and the related chemical physical properties.

EPR, ESCA, and Magnetic Susceptibility Data. There is strong evidence for the presence of Ru(IV) in **I**. The EPR spectra of different samples of **I** show in all cases the presence of only one peak of very weak intensity at the highest instrumental gain, at $g \sim 2.00$, certainly attributable to the presence of traces of paramagnetic contaminants, normally present in phthalocyanine compounds. This means that the oxidation process associated with the insertion of oxygen into the oligomer *is not* ligand centered. Rather, it takes place at the expense of the ruthenium centers, which formally must be assigned the +4 oxidation state in order to justify the overall neutral nature of the aggregate. The presence of Ru(IV) is confirmed by the room-temperature magnetic susceptibility measurements. In fact, several samples of **I** show substantial diamagnetism, in keeping with the presence of Ru(IV) in a low-spin state; some residual paramagnetism, observed in most cases ($\mu_{eff} = 0.0-0.8\ \mu_B$), is certainly contributed by the residual unchanged $(PcRu)_2$ and traces of unknown contaminants. It is significant that the magnetic behavior of **I** parallels that observed for Ru(IV) in **II**. To our knowledge, **I** is the first reported ruthenium phthalocyanine derivative containing Ru in the oxidation state +4.

Figure 6 shows the ESCA (XPS) spectra of **I** and its precursor $(PcRu)_2$ in the energy range of the Ru(3d) and C(1s) levels. The two spectra are clearly different in the 280−283 eV region. Ru(II) in $(PcRu)_2$ shows a peak at 281 eV. The spectrum of **I** shows a peak at higher energy (>282 eV). Although the XPS spectrum is a response of the surface of the sample, it clearly indicates a variation toward higher oxidation states in going from $(PcRu)_2$ to **I**. A precise assignment of the oxidation state of ruthenium on the basis of the position of the peak in the ESCA spectrum of **I** appears difficult, since scarce data are present in the literature for Ru(III) or Ru(IV) in similar macrocycles.

IR, Raman, and Electrical Conductivity Measurements. The IR spectrum of **I** has been explored in the range 4000−200 cm^{-1}. It shows a very broad exciton absorption, spreading over almost all the range (Figure 7), typical of highly electrically

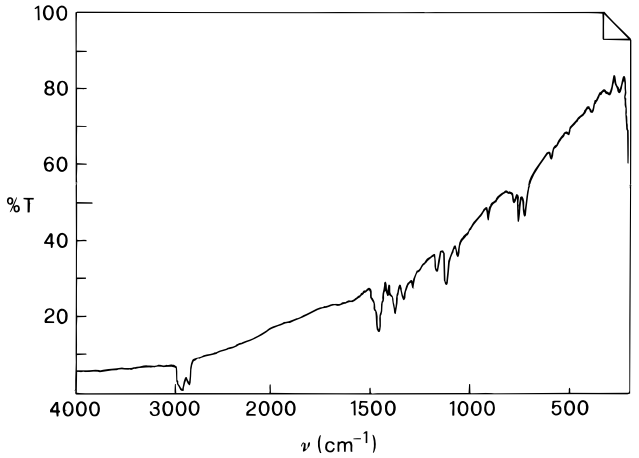

Figure 7. Nujol mull IR spectrum of **I** in the region 4000−200 cm^{-1}.

conductive systems. The characteristic skeletal Pc absorptions are all clearly detectable, although weak in intensity, a fact which is commonly associated with the presence of the exciton band. The M−O−M antisymmetric stretching is normally observed in the region 1000−800 cm^{-1} and indeed, this was the case for the materials $[(Pc)MO]_n$.[5] The IR spectrum of **I** shows no absorptions in this region, with the exception of the skeletal Pc vibration present at ca. 910 cm^{-1}. In an attempt to identify an absorption attributable to ν_{as}(Ru−O−Ru), **I** was prepared by using ^{18}O-enriched (70%) dioxygen. The IR spectrum of the material obtained shows no shift for any of the bands present in the region below 1000 cm^{-1}. Nor was, in this respect, any help provided by examination of the Raman spectrum in the same region. In conclusion, then, no evidence could be obtained for the presence of ν_{as}(Ru−O−Ru) in the IR and Raman spectra of **I**.

I, like $(PcRu)_2$, is also an electrically conductive material. Its measured σ_{RT} value is 1.10^{-2} Ω^{-1} cm^{-1}. It is significant that this value is much higher (10^3 times) than that of $(PcRu)_2$.[1a] This high σ_{RT} contrasts with the observed significantly longer interplanar distance for **I** (3.69 Å), with respect to the average value found for its precursor (3.36 Å),[1a] the two structures having similar developments of the linear aggregate (12 Pc units in $(PcRu)_2$, 11 in **I**) and identical alternated staggering and eclipsing arrangements of the Pc units, with close staggering angles for adjacent molecules (45° in $(PcRu)_2$, 35° in **I**). In $(PcRu)_2$ the charge transfer along the stacked material was assumed to occur by $\pi-\pi$ interactions of adjacent, though domed, Pc rings. Participation of the Ru centers in the charge transfer was instead reasonably excluded on the basis of the "internal" location within the dimer of the strongly interacting Ru couples (bond distance 2.40 Å) and of the long interdimer Ru−Ru contacts (4.32 Å). Vice versa, in **I** the role played by the central metal is certainly relevant, since the Ru(IV) ions are located in the center of the planar Pc units and are joined by Ru−O−Ru bridges, thus allowing charge transfer to take place through a $d\pi$(Ru)−$p\pi$(O)−$d\pi$(Ru) linkage. Noteworthy, for **I**, as discussed for **II**,[12] the Ru−O bond distance is indicative of the presence of considerable π-bond character in the Ru−O−Ru bond system. The suggested mechanism of charge transfer also evidently overcomes considerably the contrasting effect of the longer distance of adjacent rings, if any effect of this kind is really occurring.

Again with reference to the electrical conductivity properties, it is also quite interesting to compare the behavior of **I** with the series of the above mentioned structurally strictly related materials $[(Pc)MO]_n$, which are *nonconducting* systems, despite the fact that they have a more extended degree of polymerization and crystalline character, both features, in a comparison with **I**, favoring an enhancement of conduction. Clearly, then, the different electrical properties of **I** and the species $[(Pc)MO]_n$ cannot be explained on the basis of the structural features: (a) identical (oxidation state and location of the metal center, bridging bond system); (b) very similar (metal−oxygen bond distance, interplanar spacing); (c) not correlated, i.e. relative position of adjacent rings (staggered in **I**, but either staggered or eclipsed in the other materials). Here again, instead, determinant appears to be in **I** the presence of Ru(IV), with available d_{yz} and d_{xz} orbitals, the key for the charge transfer through the already mentioned $d\pi-p\pi-d\pi$ mechanism. Definitely, the phthalocyanine derivative **I** appears to be the first example of a metalloxane stacked material showing, though undoped, significant electrical conduction properties, with the central metal, a transition metal, playing a central role for the charge transfer. We might observe that a large number of undoped chain systems of general formula $[(Mac)M(L)]_n$ (Mac = Pc or peripherally substituted Pc, M = transition metal, L = neutral bidentate N-bases, CN^-, SCN^-) have been shown to be good electrically conducting systems.[14] In the latter, however, the concomitant contribution to conductivity of both the metal centers and the bridging ligands needs to be considered.

No changes of the structural features or of the electrical conductivity values are observed for **I** after a prolonged heating at 200−220 °C under vacuum (10^{-3} mmHg). Evidently this thermal treatment is not effective for the elimination of H_2O by condensation of the terminal OH groups. Such a condensation would increase the degree of polymerization, very likely allowing an increase of the crystalline character and of the σ_{RT} values. Most probably, because of the oligomeric nature of **I**, the condensation process is made difficult by the fact that the OH groups are not close enough to one another in the solid material. More drastic thermal conditions should then be applied for a successful attempt. For the metalloxane series $[(Pc)MO]_n$,[5] temperatures in the range 300−450 °C were used for this process, range precluded for **I** because of its above mentioned instability at temperatures above 200 °C.

The temperature dependence of σ in the range 240−40 K indicates $d\sigma/dT > 0$, which qualifies **I** as a semiconducting system. The fitting of the data by the equation $s = s_0 x \exp^{-DE/KT}$ leads to a value for the activation energy of 0.085 eV.

Behavior in H_2SO_4. The UV−visible spectrum of **I** in 96% H_2SO_4 shows a very broad absorption in the Q-band region with maximum centered at 670 nm (shoulder at ca. 780 nm), and peaks at ca. 400 and 275 nm (highest intensity). The spectrum changes completely, at 50 °C, in about 24 h, this implying practical disappearance of all initial peaks and appearance of intense peaks at 766 (narrow) and 285 nm, plus two lower intensity peaks at 343 and 686 nm. These spectral changes (shown in Figure 8) occur in two steps. The first one develops in about 2 h and mainly implies a shift of the broad peak from 670 to 690 nm (Figure 8, inset). During the following slower step, clean isosbestic points are evidenced at 810, 726, and 370 nm, proving the conversion of one clean intermediate species to a final one. Noteworthy, the final spectrum is perfectly coincident with that obtained by dissolving the precursor $(PcRu)_2$ in the same medium, either in the presence of air or in an inert atmosphere (N_2).

The features of the initial spectrum of **I** conform to expectation;[15] i.e., the broad band found at 670 nm is clearly diagnostic

(14) Hanack, M.; Lang, M. *Adv. Mater.* **1994**, *6*, 819.
(15) Cook, M. J. In *Spectroscopy of New Materials*; Clark, R. J. H., Hester, R. E., Eds.; Advances in Spectroscopy, Vol. 22; John Wiley & Sons: Chichester, U.K., 1993; Chapter 3, pp 87−150.

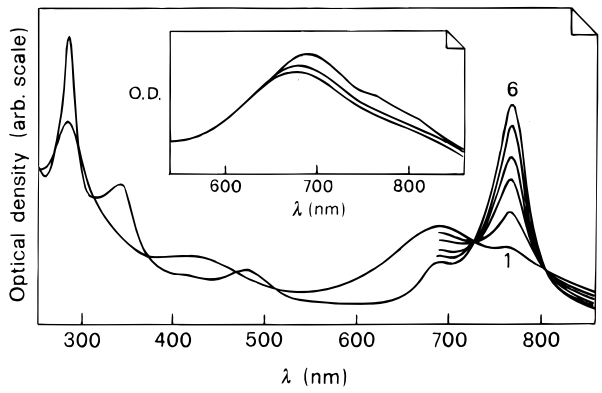

Figure 8. Spectral behavior of **I** in 96% H_2SO_4: first (inset) and second step (showing isosbestic points).

of the presence of an associated species. A similar broad absorption at ca. 680 nm is shown by the silicon oligomer $[(Pc)SiO]_n$, prepared by us as described previously,[5] when dissolved in 96% H_2SO_4. Unlike the behavior observed for **I**, however, the spectrum of the silicon material is stable with time. In solution of the same medium, instead, the analogous species $[(Pc)GeO]_n$ and $[(Pc)SnO]_n$ are unstable, suggesting the breaking of the stacked material. The instability of the M−O−M bonds in these Ge and Sn species was reasonably assigned to the insufficient protection exerted by the Pc rings to the action of the medium as a consequence of the longer M−O bonds with respect to those present in the silicon analogue. This explanation applies as well to the case of **I**, since the inter-ring spacings and the Ru−O bond lengths are intermediate between those of $[(Pc)GeO]_n$ and $[(Pc)SnO]_n$. The progressive breaking of the Ru−O−Ru backbone in **I** is proved by the following observations: (i) The solid material precipitated from the H_2SO_4 solution by addition of cold water about 20 min after dissolution of **I** shows an IR spectrum with a considerably less intense excitonic band and more clearly detectable Pc absorptions. Conductivity measurements give for this material a σ_{RT} value of ca. 10^{-4} Ω^{-1} cm^{-1}, about 100 times smaller than that shown by **I**. Structural examination by the LAXS technique of the sample indicates appreciable differences with respect to the expectation for **I**. Rather it seems to indicate that $(PcRu)_2$ has been partly re-formed. (ii) The final UV−visible spectrum in H_2SO_4 at the end of the second step coincides with that shown by $(PcRu)_2$ in the same medium. As this spectrum has been obtained also in an inert atmosphere, then, reasonably, the final spectrum very likely belongs to a Ru(II) species. This means that the spectral changes observed for **I** imply a reversed redox process with respect to that occurring for its formation. It should be observed, however, that the solid precipitated from the solution by dilution with cold water does not exactly correspond to $[(PcRu)_2]_n$, as the solid exhibits a different IR spectrum. When dissolved in pyridine, it shows a UV−visible spectrum with a main absorption with maximum at 600 nm, i.e. different from that of $PcRu(py)_2$ (maximum at 625 nm). This material has not yet received a final unequivocal identification.

Acknowledgment. We thank Dr. G. Mattei (IMAI, CNR) for help with the Raman spectra and Dr. L. Mattogno (ICMAT, CNR) for the run of ESCA spectra and useful discussions. We also thank Dr. L. Petrilli and Mr. F. Dianetti for elemental analyses. We acknowledge financial support from the Progetto Strategico "Materiali Innovativi"of the Italian Consiglio Nazionale delle Ricerche.

IC9516673